

# Downregulation of Amyloid Precursor Protein Inhibits Neurite Outgrowth In Vitro

B. Allinquant,\* P. Hantraye,† P. Mailleux,\* K. Moya,§ C. Bouillot,\* and A. Prochiantz\*

\*Centre National de la Recherche Scientifique (CNRS) URA 1414, Ecole Normale Supérieure, 75230 Paris Cedex 05; †CNRS URA 1285 Service Hospitalier Frédéric Joliot-Commissariat à l'Énergie Atomique, Orsay; and §CNRS URA 1285 and Institut National de la Santé et de la Recherche Médicale U334, SHFJ-CEA, 91406 Orsay, France

**Abstract.** The amyloid precursor protein (APP) is a transmembrane protein expressed in several cell types. In the nervous system, APP is expressed by glial and neuronal cells, and several lines of evidence suggest that it plays a role in normal and pathological phenomena. To address the question of the actual function of APP in normal developing neurons, we undertook a study aimed at blocking APP expression using antisense oligonucleotides. Oligonucleotide internalization was achieved by linking them to a vector peptide that translocates through biological membranes. This original technique, which is very efficient and gives direct access to the cell cytosol and nucleus, allowed us to work with extracellular oligonucleotide concentrations between 40 and 200 nM. Internalization of antisense oligonucleotides overlapping the

origin of translation resulted in a marked but transient decrease in APP neosynthesis that was not observed with the vector peptide alone, or with sense oligonucleotides. Although transient, the decrease in APP neosynthesis was sufficient to provoke a distinct decrease in axon and dendrite outgrowth by embryonic cortical neurons developing in vitro. The latter decrease was not accompanied by changes in the spreading of the cell bodies. A single exposure to coupled antisense oligonucleotides at the onset of the culture was sufficient to produce significant morphological effects 6, 18, and 24 h later, but by 42 h, there were no remaining significant morphologic changes. This report thus demonstrates that amyloid precursor protein plays an important function in the morphological differentiation of cortical neurons in primary culture.

THE amyloid  $\beta$ A4 peptide-containing deposits are a constant feature of Alzheimer's disease. This peptide is produced and released by proteolytic cleavage from the transmembrane form of amyloid precursor protein (APP)<sup>1</sup> (for review see Selkoe et al., 1994). The abundance of APP in neurites surrounding amyloid-containing plaques suggests that neurons may contribute to  $\beta$ A4 deposition (Martin et al., 1991; Cras et al., 1991). In the normal brain, the precise role of APP in neurons remains unknown; however, in vitro studies have shown that the protein can promote neurite outgrowth and stimulate cell adhesion to substrate in PC12 and in Neuro-2A cells (Schubert et al., 1989a; Breen et al., 1991). In vivo, the protein is rapidly transported down the axons to terminals where it has been observed at the synapse, and the developmental time course of some isoforms

is associated with axon elongation, while other isoforms are correlated with synaptogenesis (Moya et al., 1994; Koo et al., 1990; Schubert et al., 1991; Sisodia et al., 1993).

Several functional domains have been identified on the extracellular portion of APP, one of which is involved in the triggering of fibroblast proliferation (Saitoh et al., 1989; Nionomya et al., 1993), and another of which has been implicated in calcium regulation (Mattson et al., 1993). The latter finding is of particular interest since calcium currents can modulate neurite elongation through the activation of distinct kinases present in growth cones (Davenport et al., 1993). APP is also involved in interactions with extracellular matrix components, including laminin, a molecule widely expressed during ontogenesis in all parts of the nervous system (Schubert et al., 1989b; Klier et al., 1990; Small et al., 1992; Kibbey et al., 1993). The recent characterization of an APP heparin-binding domain that interacts with heparan sulfate proteoglycans further supports a role for APP in neurite outgrowth through specific interactions with extracellular matrix molecules (Schubert et al., 1989b; Koo et al., 1993; Small et al., 1994). Taken together, the results suggest that this transmembrane molecule may be part of an adhesion/transduction system involved in cell-cell and/or cell-matrix interactions.

Address correspondence to A. Prochiantz, Centre National de la Recherche Scientifique URA 1414, Ecole Normale Supérieure, 46 rue d'Ulm, 75230 Paris Cedex 05, France. Tel. (33) 1 44 32 39 26. Fax: (33) 1 44 32 39 88. E-mail: prochian@wotan.ens.fr.

1. *Abbreviations used in this paper:* APP, amyloid precursor protein; ONS, oligonucleotides; MTT, 3-(4,5-dimethylthiazol-2-yl)-2,5-diphenyl tetrazolium bromide; NCAM, neural cell adhesion molecule.

Recently, we reported that in differentiating cortical neurons *in vitro*, transmembrane APP can associate with the cytoskeleton. We also observed that APP is present in all neuronal compartments, but that axons and cell bodies differ from the dendrites by the presence of a pool of transmembrane APP very close to the cell surface, although not directly exposed to the extracellular medium. This pool, which is markedly augmented upon calcium entry, could cycle rapidly at the cell surface and regulate neurite growth by interacting transiently with components of the plasma membrane or with extracellular elements (Allinquant et al., 1994). To investigate directly a possible role of APP in neurite outgrowth by cortical neurons in culture, we have now used an original strategy that allows the rapid and efficient internalization of antisense and sense oligonucleotides (ONS). We demonstrate here that the specific inhibition of APP synthesis downregulates neurite elongation *in vitro*.

## Materials and Methods

### Primary Neuronal Cultures

Cortical neurons from embryonic day 16 rat fetuses were prepared and cultured as previously described (Lafont et al., 1993). Briefly, dissociated cells were plated  $5 \times 10^4$ /cm plastic dishes coated with 1.5  $\mu$ g/ml polyornithine for morphometric analysis, or  $10 \times 10^4$ /cm<sup>2</sup> plastic dishes for metabolic labeling. Neuronal cultures were incubated in a chemically defined medium free of serum and supplemented with hormones, proteins, and salts.

### Antisense Internalization

Two sets of antisense ONS corresponding to the sequence present in the region of the initiator codon of APP were used. The 25-mer antisense ONS (-14+11) consisting of the sequence CTGGGCAGCATCGTGATCCTGCGTG is the inverse complement of the rat sequence. Sequence data are available from EMBL/GenBank/DBJ under accession number X07648. The 15 mer used in our experiments corresponds to a truncated sequence of the 25 mer (-4+11) consisting of the sequence CTGGGCAGCATCGTG. The sequences selected did not correspond to any other sequence in the EMBL database. Antisense ONS contained an activated thiol at the 5' end, allowing the ligation of the ONS to the cysteine residues present in pAntp, the homeodomain of Antennapedia (Joliot et al., 1991a,b). Equimolar amounts of pAntp and ONS were incubated for 2 h at 37°C in buffer at a final concentration of 20 mM Hepes and 1 M NaCl. Coupled pAntp-ONS were kept at 4°C or at -20°C. All experiments were carried out with the corresponding sense ONS. In some experiments, a biotin residue was added at the 3' end of the ONS. In some cases, the ONS were coupled with the mutant pAntp50A (Le Roux et al., 1993).

The ONS alone or coupled to peptides were added to the cells 2 h after plating. The internalization was examined 2 h later by fixing the cells with methanol at -20°C for 5 min. The biotin present in the 3' end of the ONS was detected using the streptavidin-alkaline phosphatase amplification system (Vectastain; Vector Research Labs, Burlingame, CA) according to the manufacturer's instructions. Because the cells accumulate pAntp or pAntp-ONS, and because the important parameter is the amount of ONS per cell, concentrations are given in nanograms of pAntp, free or linked, for  $10^5$  cells. In our culture conditions,  $100 \text{ ng}/10^5$  cells corresponds to a concentration of 30 nM of peptide, as well as concentrations of 42 and 26 nM for the 15- and 25-mer ONS, respectively.

### Cell Viability

Cell survival was assayed by the capacity of live cells to convert soluble 3-(4,5-dimethylthiazol-2-yl)-2,5-diphenyl tetrazolium bromide (MTT) into an insoluble dark blue formazan reaction product. This test was performed according to Denizot and Lang (1986). Briefly, 10  $\mu$ l of 5 mg/ml MTT (Merck, Paris, France) in PBS-glucose was added to each well containing 0.5 ml of medium, and the cells were returned to the incubator. After 2 h at 37°C, the medium was removed, and the dark blue formazan formed was dissolved by the addition of 100  $\mu$ l of DMSO to each well. The absorbance of the reaction product was read at 570 nm.

### Morphometric Analysis

Morphometric analyses were performed on cells fixed with 2.5% glutaraldehyde in PBS for 30 min, rinsed in PBS, and stained with Toluidine blue (Lafont et al., 1993). For each condition, 100 neurons presenting at least one neurite longer than a cell diameter were digitalized and analyzed with morphological analysis software (IMSTAR, Paris, France). We measured the length of the longest neurite, the length of all neurites, and the software calculated the surface area of the cell body profile based on outline of the soma. Comparisons were made by one-way ANOVA and paired *t* tests using Statgraphics (STSC, Inc.).

### Immunoprecipitation

The cells were prepared as described above and 2 h after plating pAntp alone or pAntp-ONS were added to the culture medium at a concentration of 250 ng/ $10^5$  cells. After 1, 3, 6, and 18 h, the culture medium was replaced with a methionine-free medium, and 25  $\mu$ Ci of [<sup>35</sup>S]methionine (1,000 Ci/mmol, Amersham Corp., Arlington Heights, IL) was added. The cultures were then replaced in the incubator for 1.5 h. The cells were then treated for immunoprecipitation as described (Rousselet et al., 1988), using a polyclonal anti-APP antiserum directed against an epitope present in the COOH-terminal region (Palacios et al., 1992) kindly provided by Dr. P. Frey (Sandoz Research Institute, Berne, Switzerland). Immunoprecipitations for neural cell adhesion molecule (NCAM) were performed with a polyclonal antiserum (gift from Dr. C. Goridis (CNRS, Marseille, France)). At each time for each culture condition, the same quantity of radiolabeled proteins as determined by trichloroacetic acid precipitation was subjected to identical immunoprecipitation conditions.

For pulse-chase experiments, the neuronal cultures were labeled with 25  $\mu$ Ci of [<sup>35</sup>S]methionine for 40 min, followed by 45-, 90-, and 150-min chase periods, during which an excess of unlabeled methionine was present in the culture medium. The immunoprecipitated proteins were analyzed by PAGE. Autoradiograms were digitized using Bioprint (Vilber Lourmat, France), and densitometry was carried out using the Image program (version 1.55; National Institutes of Health, Bethesda, MD).

### Immunocytochemistry

Cells were plated onto polyornithine-coated coverslips (15  $\mu$ g/ml) at the same density used for cell viability or for morphometric analyses ( $5 \times 10^4$ /cm<sup>2</sup>), and immunocytochemistry was performed as described in Allinquant et al. (1994). We examined APP immunoreactivity in cells fixed with paraformaldehyde (4%) and permeabilized or not with the nonionic detergent Triton X-100 so as to reveal the effect of APP antisense treatment on the two populations of APP molecules described in a previous report (Allinquant et al., 1994).

To obtain a representative and comparable series of images of the APP immunofluorescence, an appropriate exposure time for cultures of a given experiment was established and used for all subsequent photos of APP-ONS sense- and antisense-treated cells. Representative series were obtained by photographing each field of view along a diameter of each coverslip.

## Results

### Internalization of ONS by Cortical Neurons in Culture

To internalize ONS into nerve cells in culture, we took advantage of a newly discovered property of pAntp, the homeodomain of the Antennapedia trans-acting protein. This 60-amino acid long peptide translocates through biological membranes, and it accumulates both in the nucleus and in the cytoplasm of all cell types tested in culture (Joliot et al., 1991a,b; Bloch-Gallego et al., 1993; Le Roux et al., 1993). The homeodomain contains a single cysteine residue between helices 2 and 3, and we used ONS bearing a biotin residue and an activated thiol in 3' and 5', respectively, the former for visualization of the ONS, and the latter to link the ONS to pAntp cysteine residue.

In absence of reducing agent, pAntp migrates as monomeric (pAntp) and dimeric forms (Di-pAntp), the latter

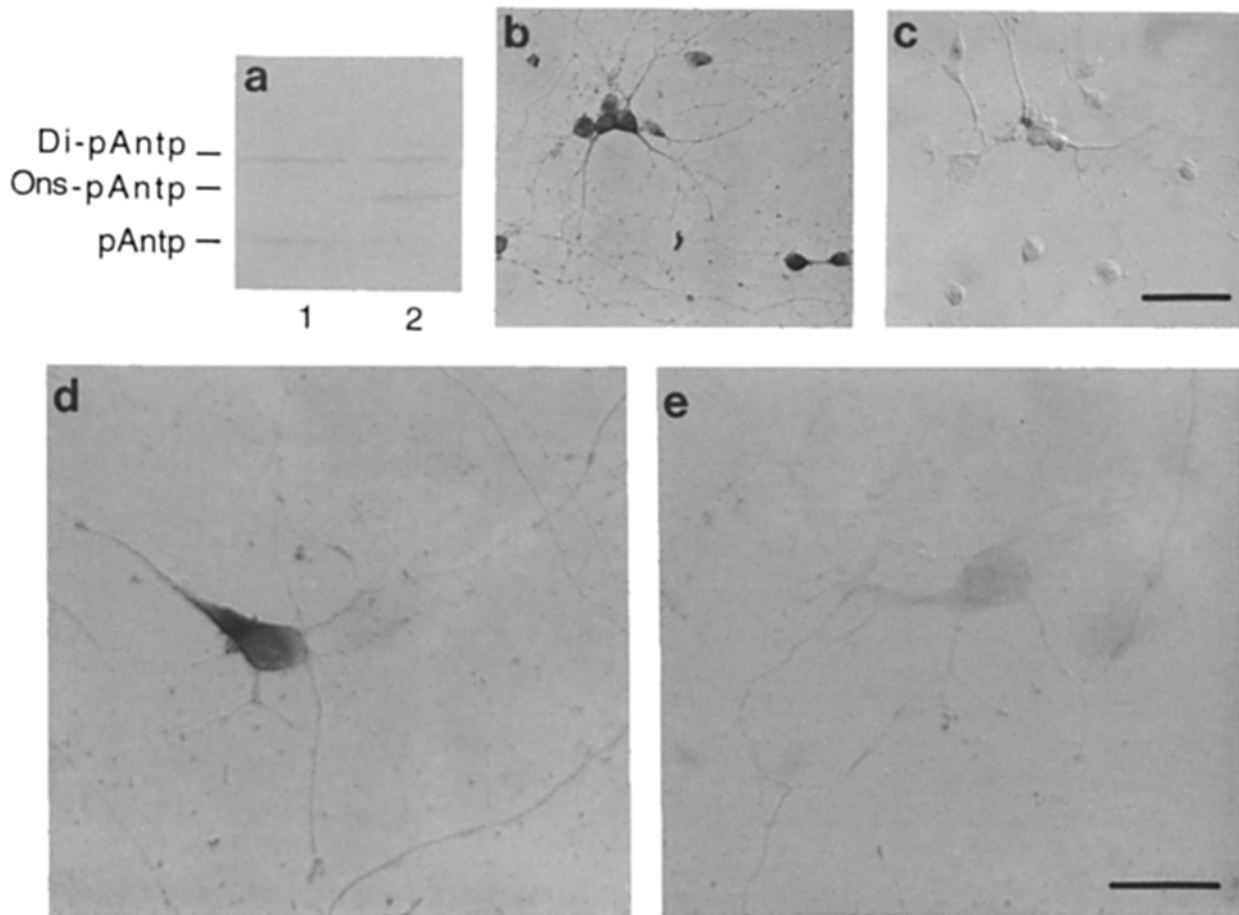


**Figure 1.** APP antisense is internalized by neurons in vitro. (a) pAntp was electrophoresed on 20% SDS-polyacrylamide gels in absence of reducing agents and monomeric (*pAntp*) and dimeric forms (*Di-pAntp*) were observed (lane 1). After coupling to the 15-mer sense ONS (lane 2), pAntp monomer band is totally shifted (*Ons-pAntp*), indicating quantitative coupling. (b–e) 250 ng of 15-mer ONS were added to  $10^5$  embryonic neurons that had been cultured for 3 d. After 2 h at 37°C, the cells were washed, fixed, and the biotinylated ONS were detected using streptavidin-alkaline phosphatase. The pAntp-coupled APP antisense ONS (b and d) is more efficiently translocated through the cell membrane and internalized than the uncoupled ONS (c and e). Bars in b and c, 10  $\mu\text{m}$ ; bar in d and e, 5  $\mu\text{m}$ .

resulting from the dimerization of the monomeric form through the cysteine residues (Fig. 1 a, lane 1). After coupling with a 15-mer ONS, the band corresponding to monomeric pAntp is no longer apparent, and a band corresponding to the peptide-ONS is observed (Fig. 1 a, lane 2, *ONS-pAntp*), showing that the coupling reaction is quantitative. Dimeric peptide with no free cysteine cannot be linked to the ONS and thus, there is no shift. Each ONS used in this study gave similar patterns of coupling and migration (not shown).

Identical amounts (100–400 ng/ $10^5$  cells) of pAntp-coupled or noncoupled ONS diluted into the medium were added to cortical cells in culture. After 2 h, the cells were washed, fixed in methanol, and internalized ONS were visualized using the biotin residue and alkaline phosphatase streptavidin. At a concentration of 250 ng/ $10^5$  cells, ONS coupled with pAntp were internalized by the cells with a very high efficiency (Fig. 1, b and d) compared to free ONS (Fig. 1, c and e). In addition, internalized pAntp-ONS are present in all compartments (cytoplasm, neurites, and nucleus). Identical

results were obtained with the 25-mer ONS and with either the sense or antisense sequences (not shown).

#### **Determination of an Efficient Concentration of pAntp-ONS**

To determine an efficient concentration of coupled ONS, we did a preliminary experiment in which we tested the effects of different amounts of coupled ONS added to the neurons 2 h after plating by measuring the surface of the soma and total neurite length 18 h later. Table I shows that these treatments did not modify the soma surface, but significantly decreased total neurite length. Controls consisted of incubating the cells with identical amounts of pAntp alone or of pAntp-sense ONS, and they showed no significant difference. The effect on neurite length was maximal at the lowest concentration tested (100 ng/ $10^5$  cells), and increasing pAntp-antisense ONS ( $\leq 400$  ng/ $10^5$  cells) did not further reduce this measure. Cell body adhesion as reflected in the soma surface measure was not altered at any concentration

**Table I. Effects of pAntp APP Antisense ONS on Neuronal Morphology**

Concentration	Soma	Total neurites length	Percent of decrease in neurite length
<i>ng/10<sup>5</sup> cells</i>	$\mu\text{m}^2$	$\mu\text{m}$	
100	pAntp	108 (4.6)	71.8 (4.4)
	pAntp-sense	ND	ND
	pAntp-a.sense	125.7 (5.8)	36.1 (3.9)
150	pAntp	130.9 (4.9)	87.3 (5.8)
	pAntp-sense	113.6 (3.6)	90.3 (5.9)
	pAntp-a.sense	111.2 (3.7)	52.6 (5.2)
200	pAntp	99.8 (5.2)	65.1 (5.1)
	pAntp-sense	ND	ND
	pAntp-a.sense	104.9 (4.9)	27.7 (2.9)
250	pAntp	113.8 (4.5)	82.7 (7.8)
	pAntp-sense	106.9 (4.5)	81.0 (7.7)
	pAntp-a.sense	106.2 (3.5)	35.7 (4.5)
300	pAntp	81.1 (2.3)	89.5 (4.9)
	pAntp-sense	84.1 (2.4)	101.5 (6.4)
	pAntp-a.sense	70.5 (1.6)	56.8 (4.7)
400	pAntp	103.4 (4.6)	73.4 (4.2)
	pAntp-sense	ND	ND
	pAntp-a.sense	107.1 (3.3)	50.4 (3.7)

pAntp alone or pAntp-ONS were added to neurons 2 h after plating, and 18 h later, soma profile surface area and total neurite length were measured. The values represent the mean (SEM) for 100 neurons in each condition. Total neurite length was significantly reduced by APP antisense at each concentration used (ANOVA,  $P < 0.001$ ). In contrast, no effect was observed on soma profile at any concentration.

of coupled antisense ONS. In addition, no change in neuronal morphology was observed in the presence of uncoupled ONS, indicating that in the experimental conditions used, the coupling of ONS to pAntp was necessary (not shown).

Although decrease in neurite length did not vary significantly between 100 and 400  $\text{ng}/10^5$  cells, in some experiments, however, we found some variability at the lowest concentration, and we thus decided to perform all further experiments at an intermediate concentration of 250  $\text{ng}$  pAntp-ONS/ $10^5$  cells. We verified that this amount of peptide or of peptide-ONS did not affect cell survival after 24 h in culture (Table II). In all of our experiments, the results obtained with the 15- and 25-mer ONS on neurite length, soma surface, and survival were virtually identical (not shown).

### pAntp-Antisense ONS Decreases APP Synthesis

In a preliminary experiment, the turnover rate of APP was estimated by pulse-chase experiments. Neurons were labeled 2 h after plating with [ $^{35}\text{S}$ ]methionine for 40 min and chased in medium containing an excess of unlabeled methionine for 45-min, 1.5-h, and 2.5-h periods before APP immunoprecipitation. The autoradiogram of Fig. 2 illustrates such an experiment and allowed calculation of a half-life of  $\sim 45$  min, consistent with that found for primary astrocytes and microglia cultured in vitro (Haass et al., 1991).

pAntp-coupled ONS were added 2 h after plating, and after 1, 3, 6, and 18 h of ONS treatment, the cells were incubated for 90 min with [ $^{35}\text{S}$ ]methionine in methionine-free

**Table II. Cell Survival Is Not Altered by pAntp or pAntp-ONS Treatment**

	Optical density $\times 10^3$
Control	68.0 (1.2)
pAntp	71.3 (0.7)
pAntp-antisense	72.2 (1.0)
pAntp-sense	73.5 (1.3)

Neurons were plated at a density of  $5 \times 10^4$  cells/ $\text{cm}^2$  and 2 h after plating, pAntp or pAntp-ONS (250  $\text{ng}/10^5$  cells) was added. 18 h later, cell viability was determined by MTT densitometry. No difference (one-way ANOVA) in survival was observed between the different conditions.

medium. For each condition (pAntp-sense ONS or -antisense ONS), the same quantity of labeled proteins, determined by trichloroacetic acid precipitable counts per minute, were subjected to immunoprecipitation with an anti-COOH-terminal APP polyclonal antibody. Sense ONS addition had no effect on APP neosynthesis at any time, and the inhibition of APP synthesis was calculated in percentage of control (sense ONS) after quantitation of the autoradiograms. As illustrated in Fig. 3 (three independent experiments), APP synthesis was markedly inhibited by 2.5 h after the addition of the antisense ONS. Inhibition of neosynthesis lasted for  $\geq 4.5$  h, and it reversed progressively with time showing a complete return to control values 7.5 h after addition of the antisense ONS.

In the same three independent experiments shown in Fig. 3, we observed no change in the neosynthesis of NCAM, another transmembrane glycoprotein involved in neurite outgrowth, 2.5 h after the addition of the APP antisense ONS. To further verify the reproducibility of the inhibition of APP neosynthesis, we performed four additional experiments and calculated that the decrease in APP neosynthesis after 2.5 h was  $27.3 \pm 4.5\%$  ( $n = 7$ ; 250  $\text{ng}/10^5$  cells). It can thus be concluded that the coupled antisense at a concentration of 250  $\text{ng}/10^5$  cells has a significant and specific effect on APP neosynthesis that can last during  $\geq 4.5$  h after its addition to the culture medium.

The decrease in APP synthesis 2 h after the addition of pAntp-antisense ONS could be visualized by immunocytochemistry experiments in which all fields along a diameter were photographed with the same exposure time. Fig. 4, which was constructed by taking every fourth field, illus-

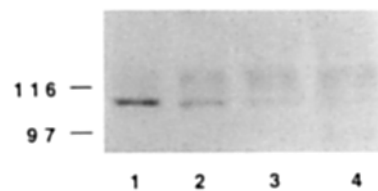


**Figure 2.** Pulse-chase labeling of primary neuronal cultures. 2 h after plating, cells were pulse labeled with 25  $\mu\text{Ci}$  of [ $^{35}\text{S}$ ]methionine for 40 min (lane 1) and were then chased in medium containing an excess of unlabeled methionine for 45 min (lane 2), 1.5 h (lane 3), and 2.5 h (lane 4). APP was then immunoprecipitated from cell lysates and separated by PAGE. Densitometric scanning of the autoradiograms allowed us to calculate an estimated half-life of the protein of  $\sim 45$  min.

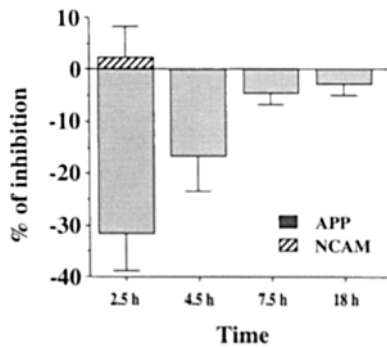


**Figure 3.** APP synthesis is inhibited by internalized APP antisense ONS. 250 ng/10<sup>6</sup> cells of pAntp-antisense or sense were added 2 h after plating, and the cells were incubated for 1, 3, 6, or 18 h. The cells were then metabolically labeled by the addition of 25  $\mu$ Ci [<sup>35</sup>S]methionine per dish for 1.5 h. APP and/or NCAM were immunoprecipitated from cell lysates containing equal amounts of trichloroacetic acid precipitable radioactivity. The autoradiograms were digitized, and the density of the APP bands were determined. The percent changes in APP synthesis in the antisense-treated cultures relative to the sense-treated cultures are the mean  $\pm$ SEM of three different experiments.

trates the decrease in APP immunoreactivity. In the latter figure, the cells were fixed and permeabilized with Triton X-100, giving access to all APP compartments. Experiments in which Triton X-100 was omitted, a protocol that only allows for the detection of APP molecules present near the cell surface and that is primarily expressed in axons and cell bodies (see Discussion and Allinquant et al., 1994), demonstrated a similar inhibition (not shown). Also note that compared to controls (sense), the cells grown in the presence of the antisense have less and smaller neuritic extensions.

#### Kinetics of Neurite Inhibition

Neuronal morphology (soma surface and total neurite length) were analyzed 6, 18, 24, and 42 h after the addition of pAntp, pAntp-sense ONS, or pAntp-antisense ONS. Although neurite inhibition could be visualized already 4 h after plating (2 h after addition of the antisense, see Fig. 4), 6 h was the earliest time we could reliably quantify the length of clearly growing neurons. APP antisense ONS treatment significantly reduced total neurite length by 6 h, and this reduction remained significant at 18 and 24 h (Fig. 5, upper panel). By 42 h, there was no significant difference in total neurite length between pAntp-antisense ONS-treated cells and cells grown in presence of the sense sequence or of pAntp alone. In contrast, the surface area of the soma was not modified by pAntp-antisense ONS at any time tested (Fig. 5, lower panel). It is important to note that the neurites continued to elongate in all conditions, and that the reversibility of the effects, which correlates with the transient inhibition of APP synthesis (Fig. 3), indicates that ONS treatment had little or no toxic effects on the cells.

#### pAntp-Antisense ONS Affect All Neurites

To analyze more precisely the morphological effects of the ONS, we quantified separately the changes in the length of all neurites, the length of the longest neurite, and the length

of all other neurites. Using markers specific for the axonal and dendritic compartments (Allinquant et al., 1994), we verified that the longest neurite corresponds to the axon in 90% of the cases, and that the other neurites correspond to young dendrites (see also Lafont et al., 1993). Fig. 6 (top) shows that the growth of putative axons and dendrites was equally inhibited by the addition of pAntp-antisense ONS, and thus that APP is involved in the outgrowth of all neurites.

Since we previously demonstrated that pAntp (at higher concentrations) has a positive effect on neurite elongation, we repeated the same experiments by coupling the ONS to pAntp50A, a mutant peptide that translocates through the membranes, but that is devoid of neurotrophic effects (Le Roux et al., 1993). We found that pAntp50A-ONS and pAntp-ONS have similar effects (Fig. 6, bottom).

In all experiments, a number of live cells remain without neurites or with neurites shorter than the somatic diameter at 18 h. This number doubles in the presence of antisense. Intersections with abscissa in the distribution graphs of Fig. 6 indicate that the percentage of cells with neurites smaller than a cell diameter increases from 25 to 50%. Interestingly, at 42 h, this percentage falls to <1% in both conditions (sense and antisense, 1,700 cells examined in three independent experiments).

## Discussion

### Oligonucleotides Internalization

The technique used here to efficiently internalize ONS is based on the translocating property of the homeodomain of Antennapedia and of its third helix (Joliot et al., 1991a,b; Bloch-Gallego et al., 1993; Le Roux et al., 1993; Derossi et al., 1994). A major advantage of this technique is that translocation does not require endocytosis and, consequently, the coupled ONS are not targeted into the endosomes and lysosomes (Neckers, 1993). Although the mechanism for this translocation is still under investigation, we know from our earlier studies (Joliot et al., 1991a,b; Le Roux et al., 1993; Perez et al., 1992) that the wild-type and mutated homeodomains accumulate in both the cytoplasm and the nucleus, two locations where antisense ONS are supposed active. The high translocation efficiency allows us to achieve effective ONS concentrations without incubating the cells in large extracellular concentrations of phosphodiester or phosphorothioate ONS, which can lead to artifacts or toxicity.

A possible pitfall in the experiments presented here is that pAntp has been demonstrated to enhance the differentiation of cortical cells in culture. This is why, in all experiments, the controls always included either uncoupled pAntp or sense ONS coupled to pAntp. It is also noteworthy that the pAntp-antisense ONS is active at a peptide concentration (100 ng/10<sup>6</sup> cells) that is below the threshold concentration necessary to increase neuronal differentiation (Bloch-Gallego et al., 1993). Furthermore, active concentrations of pAntp enhance neurite growth, whereas our results with pAntp-ONS clearly have the opposite effect.

Since the APP promoter contains several putative binding sites for homeoproteins (Salbaum et al., 1988; Odenwald et al., 1989), and since it has been shown by cotransfection experiments in nonneuronal cells that the homeoprotein HoxC8 downregulates APP expression (Violette et al.,

Sense

Antisense

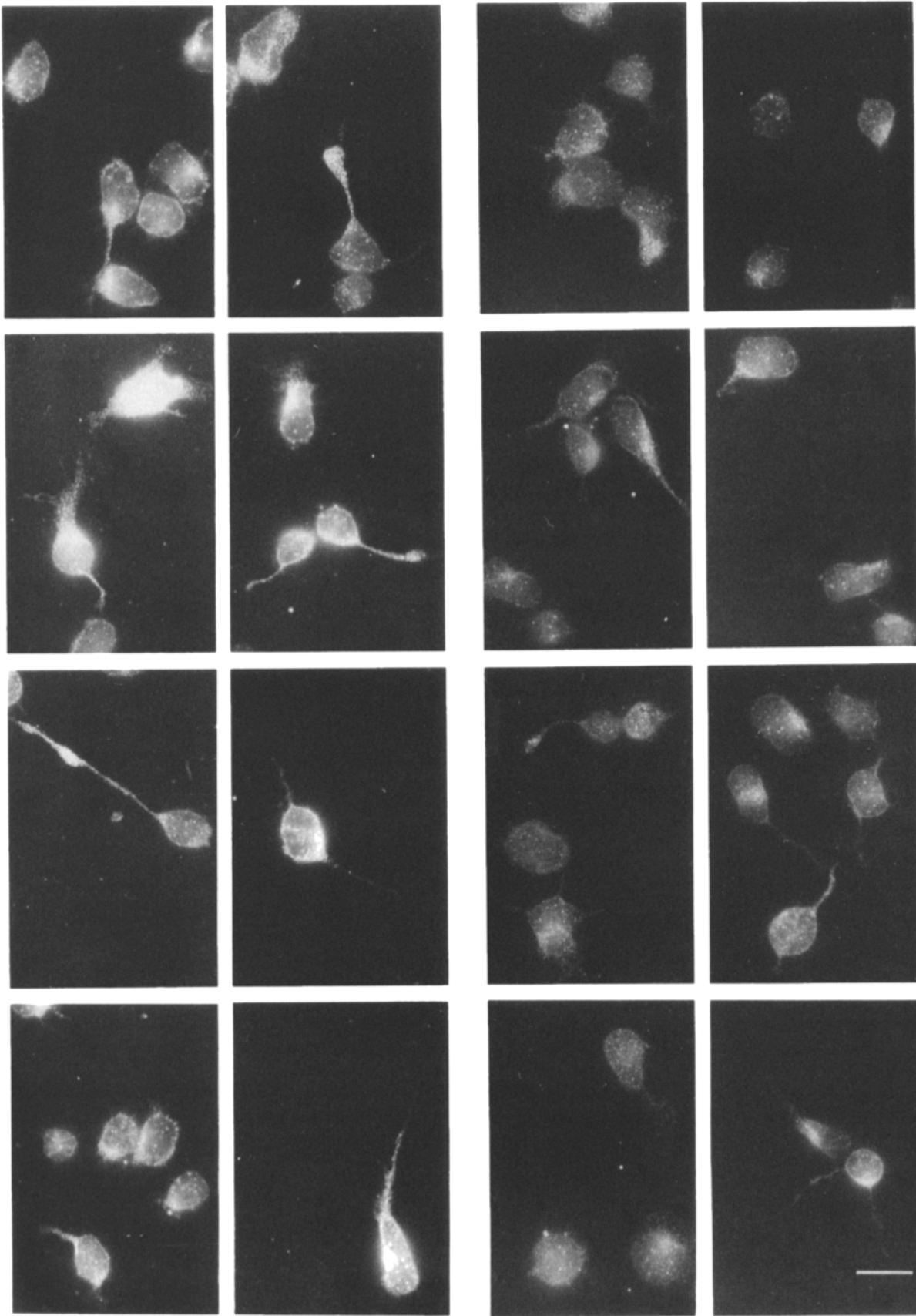


**Figure 4.** APP immunoreactivity in neuronal cultures treated with APP pAntp-ONS. pAntp-ONS was added to the culture 2 h after plating and left for another 2 h period before fixation, Triton permeabilization, and immunocytochemistry. All fields along a diameter line were photographed using the same exposure time. This figure, which presents every fourth microphotograph along the diameter for sense- and antisense-treated cultures, illustrates the decrease in APP immunostaining after antisense addition. Similar results have been observed in three experiments performed in triplicate, as well as for permeabilized (paraformaldehyde fixation and detergent) and nonpermeabilized cells (paraformaldehyde fixation, no detergent). Bar, 5  $\mu$ m.

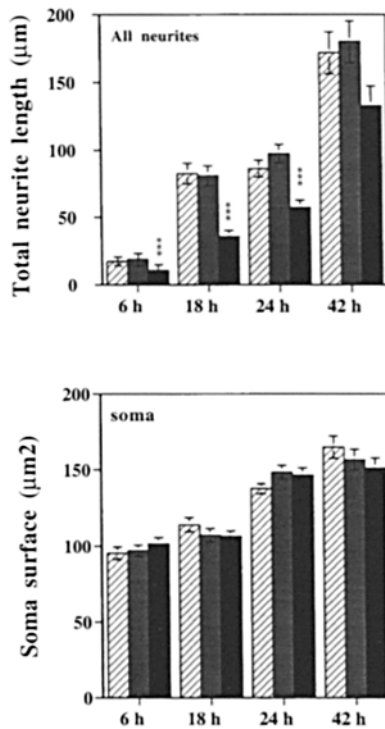
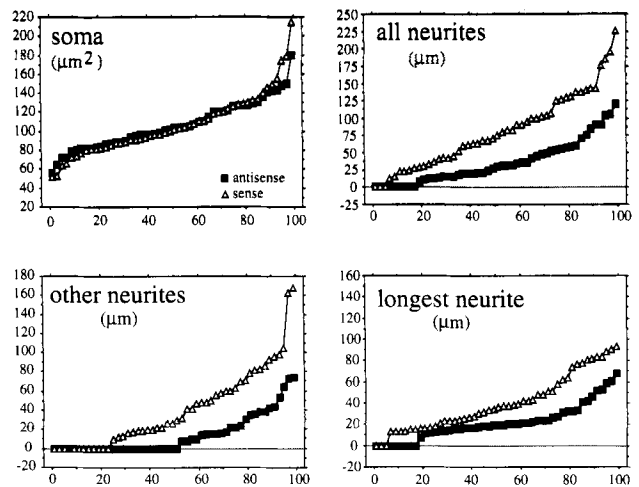


**Figure 5.** APP antisense inhibits neurite outgrowth. pAntp alone (hatched bars), coupled to APP sense ONS (gray), or to APP antisense ONS (black) were added to the neurons 2 h after plating ( $250 \text{ ng}/10^5 \text{ cells}$ ). 6, 18, 24, or 42 h later, morphological traits were analyzed. Compared to pAntp alone or to pAntp-sense, total neurite length (upper panel) was significantly reduced ( $P < 0.001$ ) in the cells treated with APP antisense sequence after 6, 18, and 24 h. Note that although APP antisense treatment reduced neurite length, it did not block the growth of the neurites since total length did increase over time, albeit more slowly. By 42 h, the difference between pAntp-antisense and the other conditions was no longer significant. APP antisense treatment had no effect on the soma profile area (lower panel).

1992), one could imagine that pAntp itself alters APP synthesis. We feel that a direct effect of pAntp on APP expression is not a likely explanation for our results since the control experiments always included pAntp alone or pAntp-sense ONS, and these conditions did not alter APP synthesis nor neuronal morphology. Furthermore, APP antisense linked to pAntp50A, which translocates through the membranes, but is unable to bind homeoprotein target sequences and is devoid of activity (Le Roux et al., 1993) lead to the same effects as pAntp-antisense ONS. We conclude that reduced neurite elongation is related to the inhibition of APP synthesis by the antisense ONS.

It should also be pointed out that we have always reported the amount of coupled oligonucleotides in nanograms of peptide per  $10^5$  cells. This dose unit mode is the most relevant since the peptide is actively concentrated with high efficiency by the cells, and the important parameter is thus the amount of oligonucleotide per cell rather than its external concentration. We need to stress, however, that given a total volume of 0.5 ml/dish, most experiments were achieved at a concentration of 75 nM ( $250 \text{ ng}/10^5 \text{ cells}$ ), the minimum active

## pAntp-coupled



## pAntp50A-coupled

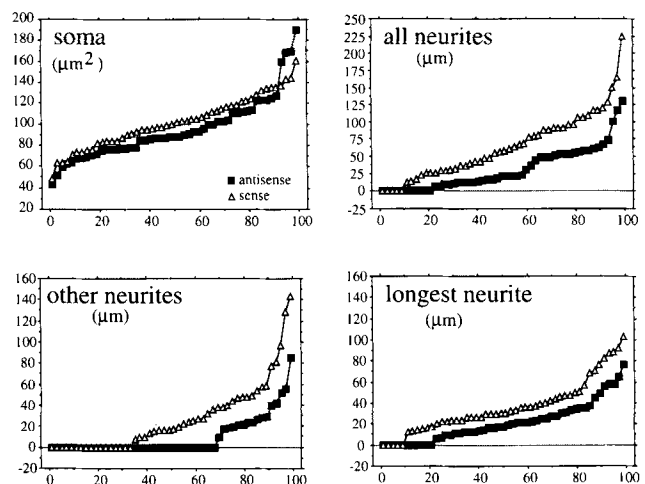


**Figure 6.** APP antisense inhibits the outgrowth of all neurites.  $250 \text{ ng}/10^5 \text{ cells}$  of antisense (filled squares) or sense (open triangles) ONS coupled to pAntp (upper part) were added to neurons 2 h after plating. Soma profile surface area, total neurite length, longest neurite length, and the length of all other neurites excluding the longest were measured 18 h later. Cumulative distributions show a marked decrease in neurite length, regardless of neurite type. When the ONS were coupled to pAntp50A, a mutated form that translocates across membranes but does not bind to genomic targets, similar results were observed for all parameters (lower part).

concentration being 30 nM ( $100 \text{ ng}/10^5 \text{ cells}$ ). These numbers can be compared to the 50–200 μM concentrations necessary to obtain biological effects when noncoupled antisense phosphodiester ONS are used (Ferreira et al., 1992; Aigner and Caroni, 1993). Finally, concerning this new technique for oligonucleotide internalization, we have internalized oligonucleotides  $\geq 45$  mer without loss of efficiency and shown that the oligonucleotides are freed from the peptide vector within 2 h after internalization by the reduction of the S-S linkage (unpublished results).

### Inhibition of APP Synthesis and Neurite Growth

The inhibition of APP synthesis was analyzed at the level of newly synthesized molecules. We found that the inhibition is very rapid and remains significant for  $\geq 4.5$  h with a complete return to control levels of neosynthesis 7.5 h after antisense addition. This transient effect on APP synthesis is best explained by the instability of phosphodiester oligonucleotides within the cells. Although we have not quantified the half-life of the oligonucleotides within the cells, the fact that a prolonged inhibition of APP neosynthesis could be obtained with only 100 nM of antisense indicates a half life much longer than the 10 min reported in other studies (Lallier and Bonner-Fraser, 1993). This prolonged half-life probably results from direct targeting of the ONS into the cytoplasm without passage into the endoplasmic and lysosomal compartments.

It is noteworthy that, in spite of a transient inhibition of APP synthesis, the antisense had long-lasting effects on neurite growth ( $\geq 24$  h). A possible explanation is that, because of the rapid turnover of the molecule (half-life of 45 min), the strong and rapid decrease in APP expression observed during the first 4.5 h is sufficient to maintain the protein concentration below a critical threshold for activity. The fact that the percentages of inhibition are very similar during the first 24 h, as well as the absence of further effects when antisense concentrations are raised to 400 ng/10<sup>5</sup> cells, are also in favor of the existence of a critical threshold. In this context, it is noteworthy that the existence of concentration thresholds has been shown for NCAM (Doherty et al., 1990) and P-cadherin (Steinberg and Takeichi, 1994).

It is important to keep in mind that the inhibition of neurite growth is reversed after 42 h, indicating that sufficient concentration of APP has been attained and that the health of the cells was not compromised by the ONS treatment. At no concentration were we able to block >40–50% of neurite extension. This is consistent with experiments showing that total inhibition of neurite growth requires antibodies directed against several cell surface adhesion molecules (Tomaselli et al., 1986).

APP antisense-induced inhibition of neurite growth affected all neurites, both axons and dendrites. Although we did not characterize the two types of neurites throughout the present study, we have previously shown that the longest neurite expresses the axonal protein tau and a neurofilament isoform highly enriched in the axonal compartment (Penny-packer et al., 1991; Lafont et al., 1992; Allinquant et al., 1994). In contrast to the smallest neurites, the longest neurites (i.e., axons) contained only small amounts of MAP2, a dendrite-enriched, microtubule-associated protein (Matus et al., 1986). In addition, in several other studies using the same markers, we showed that the longest neurite is an axon in >90% of the cells analyzed (Lafont et al., 1993).

The present results demonstrate that APP is involved in the regulation of neurite growth and might contribute to provide an indication of its mode of action. Interestingly, we noticed that the size of the soma and thus the spreading of the cell bodies on the polyornithine substratum was not modified through APP inhibition, suggesting that the effects on neurite growth are not caused by a global change in cell-substratum adhesion. The results, obtained for the first time with neurons in primary cultures, are in agreement with those of

other investigators on neuroendocrine cell lines (Milward et al., 1992; Kibbey et al., 1993). APP might thus locally interfere with adhesion and/or serve as an adhesion/transduction signal.

However, in a previous study, we demonstrated that most APP molecules are intracellular and associated with the cytoskeleton, and we proposed that a pool closest to the cell surface, highly enriched in the axons and soma, and regulated by calcium influx, could recycle rapidly with the cell surface (Allinquant et al., 1994). In view of those results, should APP action be caused primarily by interaction with an extracellular component, APP antisense ONS would preferentially inhibit axonal elongation and not that of all neurites. This is not what we observed in the present study since the decrease of APP immunoreactivity in the two pools correlates with a decrease in the initiation and elongation rate of all neurites.

Further experiments will thus be necessary to investigate whether neurite inhibition occurs through interference with a function of APP related to *cis*- or *trans*-interactions occurring at the level of the surface or to interactions with intracellular elements, in particular elements of distinct transduction pathways and components of the cytoskeleton (Nishimoto et al., 1993; Allinquant et al., 1994).

We are grateful to Drs. P. Frey and C. Goridis, who generously contributed the APP COOH-terminal and NCAM antibodies, respectively. This work was supported by Centre National de la Recherche Scientifique, Ecole Normale Supérieure, and grants from Direction des Recherches et Etudes Techniques (DRET 92-141) and Institut National de la Santé et de la Recherche Médicale (CRE 930807). Pierre Mailloux is an IPSEN foundation fellow.

Received for publication 27 June 1994 and in revised form 24 November 1994.

### References

- Aigner, L., and P. Caroni. 1993. Depletion of 43-kD growth-associated protein in primary sensory neurons leads to diminished formation and spreading of growth cones. *J. Cell Biol.* 123:417–429.
- Allinquant, B., K. L. Moya, C. Bouillot, and A. Prochiantz. 1994. Amyloid precursor protein in cortical neurons: co-existence of two pools differentially distributed in axons and dendrites and association with cytoskeleton. *J. Neurosci.* 14:6842–6854.
- Bloch-Gallego, E., I. Le Roux, A. H. Joliot, M. Volovitch, C. E. Henderson, and A. Prochiantz. 1993. Antennapedia homeobox peptide enhances growth and branching of embryonic chicken motoneurons in vitro. *J. Cell Biol.* 120:485–492.
- Breen, K. C., M. Bruce, and B. H. Anderson. 1991.  $\beta$  amyloid precursor protein mediates neuronal cell-cell and cell-surface adhesion. *J. Neurosci. Res.* 28:90–100.
- Cras, P., M. Kawai, D. Lowery, P. Gonzalez-de Whitt, B. Greenberg, and G. Perry. 1991. Senile plaque neurites in Alzheimer's disease accumulate amyloid precursor protein. *Proc. Natl. Acad. Sci. USA.* 88:7552–7556.
- Davenport, R. W., P. Dou, V. Rehder, and S. B. Kater. 1993. A sensory role for neuronal growth cone filopodia. *Nature (Lond.)* 361:721–724.
- Denizot, F., and R. Lang. 1986. Rapid colorimetric assay for cell growth and survival. *J. Immunol. Methods.* 89:271–277.
- Derossi, D., A. H. Joliot, G. Chassaing, and A. Prochiantz. 1994. The third helix of the antennapedia homeodomain translocates through biological membranes. *J. Biol. Chem.* 269:10444–10450.
- Doherty, P., M. Fruns, P. Seaton, G. Dickson, C. H. Barton, T. A. Sears, and F. S. Walsh. 1990. A threshold effect of the major isoforms of NCAM on neurite outgrowth. *Nature (Lond.)* 343:464–466.
- Ferreira, A., J. Nielas, R. D. Vale, G. Banker, and K. S. Kosik. 1992. Suppression of kinesin expression in cultured hippocampal neurons using antisense oligonucleotides. *J. Cell Biol.* 117:595–606.
- Haass, C., A. Y. Hung, D. J. Selkoe. 1991. Processing of  $\beta$ -amyloid precursor protein in microglia and astrocytes favors an internal localization over constitutive secretion. *J. Neurosci.* 11:3783–3793.
- Joliot, A., C. Pernelle, H. Deagostini-Bazin, and A. Prochiantz. 1991a. Antennapedia homeobox peptide regulates neural morphogenesis. *Proc. Natl. Acad. Sci. USA.* 88:1864–1868.



- Joliot, A. H., A. Triller, M. Volovitch, C. Pernelle, and A. Prochiantz. 1991b.  $\alpha$ -2,8-polysialic acid is the neuronal surface receptor of antennapedia homeobox peptide. *New Biol.* 3:1121-1134.
- Kibbey, M. C., M. Jucker, B. S. Weeks, R. L. Neve, W. E. Van Nostrand, and H. K. Kleinman. 1993.  $\beta$ -amyloid precursor protein binds to the neurite-promoting IKVAV site of laminin. *Proc. Natl. Acad. Sci. USA.* 90: 10150-10153.
- Klier, F. G., G. Cole, W. Stallcup, and D. Schubert. 1990. Amyloid  $\beta$ -protein precursor is associated with extracellular matrix. *Brain Res.* 515:336-342.
- Koo, E. H., S. S. Sisodia, D. R. Archer, L. J. Martin, A. Weidemann, K. Beyreuther, P. Fischer, C. L. Masters, and D. L. Price. 1990. Precursor of amyloid protein in Alzheimer disease undergoes fast anterograde axonal transport. *Proc. Natl. Acad. Sci. USA.* 87:1561-1565.
- Koo, E. H., L. Park, and D. J. Selkoe. 1993. Amyloid  $\beta$ -protein as a substrate interacts with extracellular matrix to promote neurite outgrowth. *Proc. Natl. Acad. Sci. USA.* 90: 4748-4752.
- Lafont, F., M. Rouget, A. Triller, A. Prochiantz, and A. Rousset. 1992. In vitro control of neuronal polarity by glycosaminoglycans. *Development (Camb.).* 114:17-29.
- Lafont, F., M. Rouget, A. Rousset, C. Valenza, and A. Prochiantz. 1993. Specific responses of axons and dendrites to cytoskeleton perturbations: an in vitro study. *J. Cell Sci.* 104:433-443.
- Lallier, T., and M. Bonner-Fraser. 1993. Inhibition of neural crest cell attachment by integrin antisense oligonucleotide. *Science (Wash. DC).* 259: 692-695.
- Le Roux, I., A. H. Joliot, E. Bloch-Gallego, A. Prochiantz, and M. Volovitch. 1993. Neurotrophic activity of the Antennapedia homeodomain depends on its specific DNA-binding properties. *Proc. Natl. Acad. Sci. USA.* 90: 9120-9124.
- Martin, L. J., S. S. Sisodia, E. H. Koo, L. C. Cork, T. L. Dellovade, A. Weidemann, K. Beyreuther, C. Masters, and D. L. Price. 1991. Amyloid precursor protein in aged nonhuman primates. *Proc. Natl. Acad. Sci. USA.* 88:1461-1465.
- Mattson, M. P., B. Cheng, A. R. Culwell, F. S. Esch, I. Lieberburg, and R. E. Rydel. 1993. Evidence for excitoprotective and intraneuronal calcium-regulating roles for secreted forms of the  $\beta$ -amyloid precursor protein. *Neuron.* 10:243-254.
- Matus, A., R. Bernhardt, R. Bodmer, and D. Alaimo. 1986. Microtubule-associated protein 2 and tubulin are differently distributed in the dendrites of developing axons. *Neurosci.* 17:371-389.
- Milward, E. A., R. Papadoulos, S. J. Fuller, R. D. Moir, D. Small, K. Beyreuther, and C. L. Masters. 1992. The amyloid protein precursor of Alzheimer's disease is a mediator of the effects of nerve growth factor on neurite outgrowth. *Neuron.* 9:129-137.
- Moya, K. L., L. I. Benowitz, G. E. Schneider, and B. Allinquant. 1994. The amyloid precursor protein is developmentally regulated and correlated with synaptogenesis. *Dev. Biol.* 161:597-603.
- Neckers, L. M. 1993. The use of antisense oligonucleotides in neural systems. *Neuroprotocols.* 2:3-7.
- Ninomiya, H., J. M. Roch, M. P. Sundsmo, D. A. C. Otero, and T. Saitoh. 1993. Amino acid sequence RERMS represent the active domain of amyloid  $\beta$ /A4 protein precursor that promotes fibroblast growth. *J. Cell Biol.* 121:879-886.
- Nishimoto, I., T. Okamoto, Y. Matsuura, S. Takahashi, T. Okamoto, Y. Murayama, and E. Ogata. 1993. Alzheimer's amyloid protein precursor complexes with brain GTP-binding protein  $G_0$ . *Nature (Lond.).* 362:75-79.
- Odenwald, W. F., C. F. Taylor, F. J. Palmer-Hill, V. Friedrich, M. Tani, and R. A. Lazzarini. 1989. Expression of a homeodomain protein in noncontact-inhibited cultured cells and post-mitotic neurons. *Genes Dev.* 3:158-172.
- Palacios, G., J. M. Palacios, G. Mengod, and P. Frey. 1992. Amyloid precursor protein localization in the Golgi apparatus in neurons and oligodendrocytes. An immunocytochemical structural and ultrastructural study in normal and axotomized neurons. *Mol. Brain Res.* 15:195-206.
- Pennypacker, K., I. Fischer, and P. Levitt. 1991. Early in vitro genesis and differentiation of axons and dendrites by hippocampal neurons analyzed quantitatively with neurofilament-H and microtubule-associated protein 2 antibodies. *Exp. Neurol.* 111:25-35.
- Perez, F., A. Joliot, E. Bloch-Gallego, A. Zahraoui, A. Triller, and A. Prochiantz. 1992. Antennapedia homeobox as a signal for the cellular internalization and nuclear addressing of a small exogenous peptide. *J. Cell Sci.* 102:717-722.
- Rousset, A., L. Fetter, B. Chamak, and A. Prochiantz. 1988. Rat mesencephalic neurons in culture exhibit different morphological traits in the presence of media conditioned on mesencephalic or striatal astroglia. *Dev. Biol.* 129:495-504.
- Saitoh, T., M. Sundsmo, J. M. Roch, N. Kimura, G. Cole, D. Schubert, T. Oltersdorf, and D. B. Schenk. 1989. Secreted form of amyloid  $\beta$  protein precursor is involved in the growth regulation of fibroblasts. *Cell.* 58: 615-622.
- Salbaum, J. M., A. Weidemann, H.-G. Lemaire, C. L. Masters, and K. Beyreuther. 1988. The promoter of Alzheimer's disease amyloid A4 precursor gene. *EMBO (Eur. Mol. Biol. Organ.) J.* 7:2807-2813.
- Schubert, D., L. W. Jin, T. Saitoh, and G. Cole. 1989a. The regulation of amyloid  $\beta$  protein precursor secretion and its modulatory role in cell adhesion. *Neuron.* 3:689-694.
- Schubert, D., M. La Corbiere, T. Saitoh, and G. Cole. 1989b. Characterization of an amyloid  $\beta$  precursor protein that binds heparin and contains tyrosine sulfate. *Proc. Natl. Acad. Sci. USA.* 86:2066-2069.
- Schubert, W., R. Prior, A. Weidemann, H. Dirksen, G. Multhaup, C. L. Masters, and K. Beyreuther. 1991. Localization of Alzheimer  $\beta$ A4 amyloid precursor protein at central and peripheral synaptic sites. *Brain Res.* 563:184-194.
- Selkoe, D. J. 1994. Normal and abnormal biology of the  $\beta$ -amyloid precursor protein. *Annu. Rev. Neurosci.* 17:489-517.
- Small, D. H., V. Nurcombe, R. Moir, S. Michaelson, D. Monard, K. Beyreuther, and C. L. Masters. 1992. Association and release of the amyloid protein precursor of Alzheimer's disease from chick brain extracellular matrix. *J. Neurosci.* 12:4143-4150.
- Small, D. H., V. Nurcombe, G. Reed, H. Clarriss, R. Moir, K. Beyreuther, and C. L. Masters. 1994. A heparin-binding domain in the amyloid protein precursor of Alzheimer's disease is involved in the regulation of neurite outgrowth. *J. Neurosci.* 14:2117-2127.
- Sisodia, S., E. H. Koo, P. N. Hoffman, G. Perry, and D. L. Price. 1993. Identification and transport of full-length amyloid precursor proteins in rat peripheral nervous system. *J. Neurosci.* 13:3136-3142.
- Steinberg, M. S., and M. Takeichi. 1994. Experimental specification of cell sorting, tissue spreading, and specific spatial patterning by quantitative differences in cadherin expression. *Proc. Natl. Acad. Sci. USA.* 91:206-209.
- Tomaselli, K. J., L. F. Reichardt, and J. L. Bixby. 1986. Distinct molecular interactions mediate neuronal process outgrowth on nonneuronal cell surfaces and extracellular matrices. *J. Cell Biol.* 103:2659-2672.
- Violette, S. M., C. S. Shashikant, J. M. Salbaum, H.-G. Belting, J. C. H. Wang, and F. H. Ruddle. 1992. Repression of the  $\beta$ -amyloid gene in a Hox-3.1 producing cell line. *Proc. Natl. Acad. Sci. USA.* 89:3805-3809.